

# Biochemical Analyses of Male Rat's Serum Administered Dexamethasone and Green Synthesis Cerium Oxide Nanoparticles Treatment

Ruaa M. Ali<sup>1</sup>, Nada K. Abbas<sup>1</sup>, Amal K. Abbas<sup>2</sup>, Lamia K. Abbas<sup>3</sup>

<sup>1</sup>University of Baghdad/College of Science for Women/ Physics Dept., <sup>2</sup>University of Baghdad/College of Science Biology Dept., <sup>3</sup>University of Baghdad/college of Science/ Physics Dept.

## Abstract

Current research involves preparing cerium oxide nanoparticles using simple, environmental- friendly green synthesis approach via fresh green tea leaf extract (*Camellia sinensis*) as a capping and reducing agent, Ultraviolet-visible spectroscopy (UV-Vis.) is used to check the formation of nanoparticles by investigate the absorption peak and energy gap ( $E_g$ ); Maximum absorption peak was around 295nm and  $E_g$  was 4.2eV calculated using Planck's equation, X-Ray diffraction (XRD) analysis of Nano powder stated that Cerium Oxide has a cubic fluorite structure with face centered cubic (FCC) structure, blood serum glucose levels, liver functions after CeO<sub>2</sub> Nanoparticles treatment for rats were reported in this paper. Forty eight adult male rats were used and divided randomly into six groups each group has eight rats (n=8), Results stated that blood glucose levels, liver enzymes were increased in groups that injected by dexamethasone while considerably modified in rats administered by Cerium Oxide Nanoparticles.

**Keywords:** green synthesis, dexamethasone, XRD, Cerium Oxide NPs, AST.

## Introduction

Nanomaterials are the forms of matter at nanoscale. The "Building blocks" for nanomaterials consist of organics, semiconductors, metals and metal oxides. Nanomaterials with structural features at the nanoscale can be found in the form of clusters, thin films, multilayer and Nano-crystalline materials which are often expressed by the dimensionality of 0, 1, 2 and 3 <sup>(1)(2)</sup>, The synthesis of nanomaterials is of present concern due to their huge applications in medicine and many other fields <sup>(3)</sup>, commonly, most of these applications are due to the reality that the Nanometer scale has significantly different characteristics compared to the bulk state. the nanoparticles have strong surface bonds, the high surface-volume ratio in Nanoparticles is the main reason for a structural deformation that can change the physical properties of nanoparticles <sup>(4)</sup>.

The most popular complications of hyperglycemia are the generation of (ROS) reactive oxygen species <sup>(5)</sup>. Reactive oxygen species can cause serious harm to  $\beta$ -cells and insulin resistance <sup>(6)</sup>. Hyperglycemia characterized by increases the percentage of metabolism and enzyme failure of elevated oxidative stress caused by beta cells failure in the pancreas <sup>(7)</sup>. Using plants extract is one of the latest techniques used to synthesize nanoparticles. Many metal nanoparticles were produced this way <sup>(8)</sup>, Biosynthetic pathways can provide Nanoparticles of a better defined size and morphology than some of the physicochemical preparation techniques. Plant extracts can behave both as reducing agents and as stabilizing agents in the synthesis of Nanoparticles <sup>(9)</sup>.

Many researchers have defined the capacity of CeO<sub>2</sub> Nanoparticles to scavenge free radical species to behave as an antioxidant. Multiple scientists have indicated that cerium NPs behave as a mimetic of superoxide dismutase, the primary catalyst that reduces the production and damage caused by ROS to mammalian cells by converting superoxide into oxygen and hydrogen peroxide <sup>(10)</sup>.

---

**Corresponding author:**

**Nada K. Abbas,**

email: nadabbs@yahoo.com

The objective of this research is to investigate the capacity of CeO<sub>2</sub> NPs to decrease BGL, improvement liver function using biochemical assays and histological examinations.

## Materials and Method

8.68 grams of Ce(NO<sub>3</sub>)<sub>3</sub>·6H<sub>2</sub>O (0.09M) was added to 200ml of deionized water in a flask and they stirred for 5 minutes on 1,500 rpm magnetic stirrer, then gradually 20ml of previously prepared *Camellia Sinensis* leaf extract was added to the flask. At 40°C magnetic hotplate, the mixture was constantly stirred for two hours; the solution was cooled at room temperature. Blackish brown CeO<sub>2</sub> Nanoparticles were collected by centrifugation (4,000 rpm) for 15 minutes. The NPs were washed repeatedly with deionized water and dried it with hot air oven then calcined for ~5 hours at 400 °C.

### Experimental animals

Forty eight adult male Wister albino rats weighing (175-225g) and average (10-14) weeks old, the rats were housed in polypropylene cages under controlled conditions of temperatures (25±5) °C and 12/12 hours light/dark cycles, Diet and drinking water were given *ad libitum*, the animals were reared and treated in animal house of college of science, University of Baghdad.

Laboratory animals were randomly divided into six groups, each group contained eight rats (n=8) treated for 30 days, and intended as follows: the first group (G1) was served as negative control, the second group (G2) was injected intraperitoneally with (0.5 mg/kg) dexamethasone sodium phosphate, (G3 and G4) were injected intraperitoneally with (34 and 84) mg/kg CeO<sub>2</sub> Nanoparticles and (0.5 mg/kg) of dexamethasone respectively, the fifth group (G5) was injected intraperitoneally with 34 mg/kg CeO<sub>2</sub> Nanoparticles and (G6) was injected intraperitoneally with 84 mg/kg CeO<sub>2</sub> Nanoparticles.

The experimental animals in this model was fast for 24-hours, the rats were weighed and anesthetized by their inhalation in a glass dome. Animals were injected dexamethasone sodium phosphate (0.5 mg/kg) for 30 days in a single dose daily<sup>(11)</sup>. Only 30 minutes after drug administration, food and water were provided to the animals. Within 15 days of dexamethasone injection; blood glucose elevated and insulin secretion reduced these consequences of dexamethasone

were agreed with Makoto Ohneda's outcomes<sup>(12)</sup>, animals have been received (34 and 84 mg/kg) Cerium dioxide nanoparticles<sup>(13)</sup>.

### Biochemical analysis

After the exposure period end, blood sample collected from animals by heart puncture, Collected blood was centrifuged at 4000 rpm for 10 min, serum was separated for assessment of various biochemical parameter such as blood glucose level (BGL) measured by commercially available kit (Biosystem, Germany), cholesterol (TC), Triglyceride (TG), High Density Lipoprotein Cholesterol (HDL-C) and Low Density Lipoprotein Cholesterol (LDL-C) were estimated using a commercially available kit (Linear kit, Spain), serum levels Aspartate Amino transferase (AST) Alanine Amino transferase (ALT), Alkaline Phosphate (ALP) and Total Bilirubin (TB) were estimated by commercially available kit (Reflotron kit, Germany).

### Histological Examinations

Pancreatic Samples were collected from animals after organs separation and fixed in 10% buffered neutral formalin solution, dehydrated in gradual ethanol (70%), cleared in xylene, and embedded in paraffin. 5 µm thick paraffin sections were prepared and then regularly stained with Hematoxylin and Eosin (H&E)<sup>(14)</sup> and then examined microscopically.

### Statistical Analysis

The statistical analysis was performed using analysis of one way (ANOVA) variance and t-test analysis, carried out in complete randomized design. Different between means have analyzed by Least Significant differences (LSD) at (P≤0.05) and expressed as (Mean ± SE) with letters to explain the significant using the Statistical Package for Prism 8.1.2 (Version 8.1.2, Graph Pad, San Diego, CA, USA) software.

### Results and Discussion

Nano-powder structural characterization was registered by Pro Penalty CAL with Cu-Kα radiation (1.5406 Å). XRD models for prepared Cerium Nano-powder showed that the structure is polycrystalline; as synthesized CeO<sub>2</sub> showed no pure intense peaks Fig. (1a), which is caused by amorphous state. While eight diffraction peaks existed when calcined in 400°C. Eight diffraction peaks were recorded in tab. (1) proved the

cubic fluorite structure with face centered cubic (FCC) structure of  $\text{CeO}_2$  with standard data (no: 89-8436 of JCPDS card) Fig. (1b&c). No peak of any other phase was identified the sample's high purity. The diffraction peaks of  $\text{CeO}_2$  particles are quite broad, indicating

very small crystalline sizes of sample. The pure  $\text{CeO}_2$  nanoparticle's lattice parameter is  $5.412\text{\AA}$  which matches well with the bulk  $\text{CeO}_2$  lattice parameter  $a=5.411$ . Using Debye-Scherrer formula, the calculated average particle size was around  $14.29\text{ nm}$ , these findings were agreed with <sup>(15)(16)</sup>.

**Table (1): The structural XRD parameters of the calcined synthesized  $\text{CeO}_2$  Nanoparticles**

2 $\theta$ (Deg.)	G.S (nm)	FWHM (Deg.)	$d_{hkl}$ Exp.( $\text{\AA}$ )	$d_{hkl}$ standard ( $\text{\AA}$ )	(hkl)
29.575	5.77	1.412	3.124	3.018	(111)
33.134	5.77	1.412	2.706	2.701	(200)
47.5	10.4	0.760	1.913	1.912	(202)
56.80	7.2	1.094	1.631	1.619	(311)
59.5	15.8	0.500	1.562	1.551	(222)
69.1	15.8	0.500	1.352	1.358	(400)
77.08	39.7	0.200	1.241	1.236	(313)
79.5	13.9	0.570	1.209	1.204	(402)

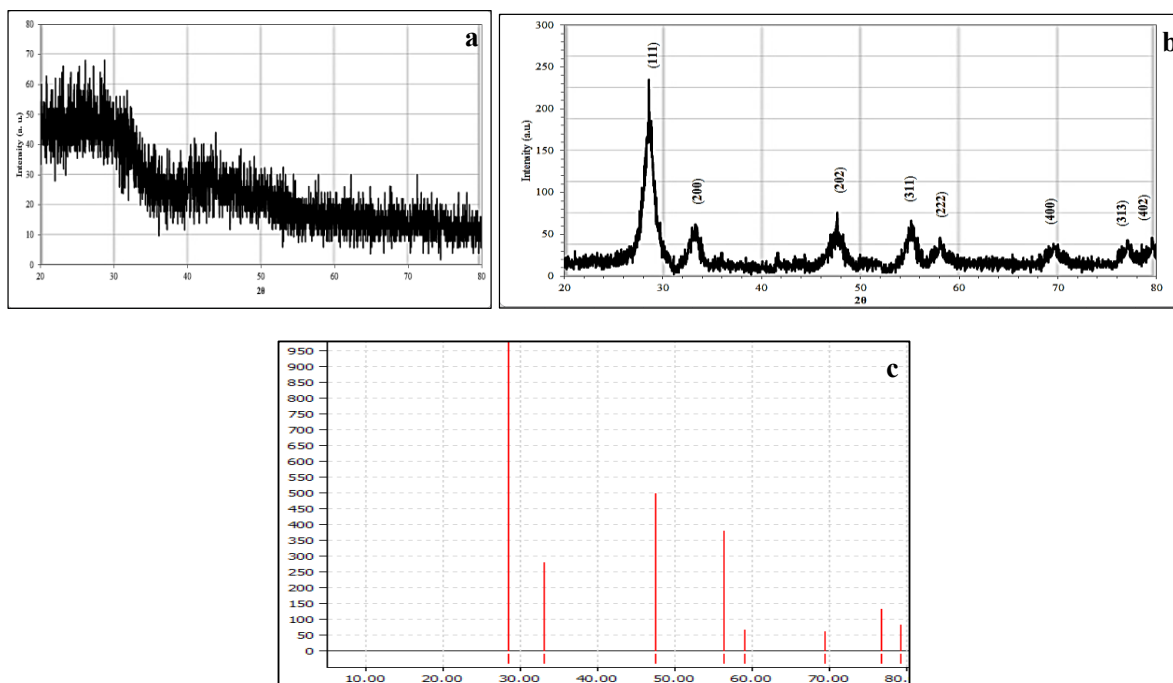


**Figure (1): (a) XRD pattern of the as synthesized  $\text{CeO}_2$  Nanoparticles (b) calcined  $\text{CeO}_2$  Nanoparticles (c) peaks positions of standard  $\text{CeO}_2$  Nanoparticles**

The optical behavior recorded by VARIAN spectrophotometer (Cary 5000 Scan), Fig. (2) Shows the appearance of single peak validates the sample purity and shows a maximum absorption peak at  $295\text{ nm}$  of green synthesized  $\text{CeO}_2$  NPs. Primarily absorption peaks were formed due to the electronic transitions and excitation of

electrons from valance band to conduction band between outer energy, The calculated Energy gap of  $\text{CeO}_2$  NPs was  $4.2\text{ eV}$  evaluated by following relation <sup>(17)</sup>, From the obtained result, the band gap energy was blue shifted which happened by the quantum confinement effect. This effect may create by oxygen vacancies present in

the inter-granular areas. Typical UV absorption peaks were also seen in previously studies<sup>(18)</sup>.

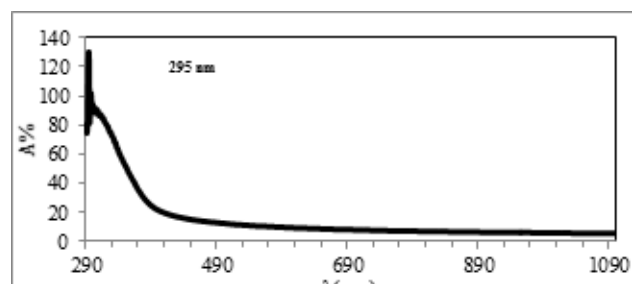


Figure (2): Absorption Spectrum of CeO<sub>2</sub> nanoparticles

The biochemical results in tab. (2) presented a significant increase in blood glucose level (BGL) in

group which treated by dexamethasone (**G2**) compared with control group (**G1**), these results similar to previous study<sup>(19)</sup> they reported that dexamethasone cause tissue damage in pancreas which leads to decrease insulin secretion from Langerhans cells. After animals treating with CeO<sub>2</sub> NPs for 30 days, there was a significant decrease ( $p \leq 0.05$ ) with blood glucose level for infected animals in **G3** and **G4** compared to **G2**. CeO<sub>2</sub> nanoparticles had the ability to reduce BGL for many reasons such as delaying or inhibiting the absorption of glucose in the intestines<sup>(20)</sup>, Stimulate insulin secretion from pancreas cells<sup>(21)</sup> or facilitate the entry of glucose into cells in fatty and muscular tissues<sup>(22)</sup>, **G5** and **G6** were found to be near the normal range of BGL.

**Table (2) Changes of Serum biochemical parameters in treated rats with CeO<sub>2</sub> Nanoparticles after 30 days, Each value represents the mean ± standard error of (n=8), The values were found to be statistically significant at  $P \leq 0.05$ , (\* $P < 0.02$ , \*\* $P < 0.001$ , \*\*\* $P < 0.0008$ , \*\*\*\* $P < 0.0001$ )**

Groups Parameters	Means± SE					
	G1	G2	G3	G4	G5	G6
BGL (mg/dL)	113.2±6.4	395.2±29.7	131.7±6**	168.5±4.7**	107.5±3.9	118.7±4.6
ALT(IU/L)	35.7±1.6	66.2±4.7	41.5±1.3*	43.2±0.8*	40.7±2.7	46.7±4.2
AST(IU/L)	27.2±4.4	48.2±3.5	34±1.7*	38.5±4.4*	40.5±1.5*	43.5±0.6*
ALP(IU/L)	151±17.8	383.2±30.7	180.2±24.9*	206.7±22.3**	149.2±26.6	206.5±40.7
TB(mg/dL)	0.33±0.01	1.42±0.08	0.36±0.02***	0.47±0.13**	0.54±0.07	0.45±0.08

Also; the results showed there was a significant increase in liver functions parameters such as ALT, AST and ALP in experimental animals compared with control group (**G1**), liver enzymes indicate the extent of liver diseases<sup>(23)</sup>, this study indicates increases of liver enzymes levels possibly due to hepatic damage, increases the activity of liver enzymes in experimental animals may reveal possible leakage of these cytoplasmic enzymes into the blood stream across damaged plasma membrane or increase synthesis of these enzymes in the liver<sup>(24)</sup>. Results of this study showed that there was a significant decreases ( $P \leq 0.05$ ) of liver enzymes in treated animals (**G3** and **G4**), the administration of CeO<sub>2</sub> Nanoparticles may reduce dexamethasone-induced hepatotoxicity in rats, the effective of CeO<sub>2</sub> Nanoparticles as an antioxidant agent by inhibiting oxidative stress formation and Reactive

Oxygen Species (ROS) due to the large surface area to volume ratio that creates reactive sites to scavenge free radicals<sup>(25)</sup>, increase of Bilirubin levels may be attributed to the changes in cell membrane permeability with change of effective stress of the membrane under the influence of the oxidative stress, or may be explained by the occurrence of obstruction in the gallbladder ducts<sup>(26)</sup>, there was a significant decrease ( $P \leq 0.05$ ) in Bilirubin levels for the treated rats, (**G5** and **G6**) had a normal liver enzymes and Bilirubin levels.

### Histological Examination

Histological section in (Fig. 3a) shows pancreatic lobules containing acini (\*), islets of Langerhans (\*\*) and unstained connective tissue septa (\*\*\*) for control

group. Fig. (3b and c) showed damage and necrosis of endocrine cells of islet (\*), Langerhans with shrinkage of islet (\*\*), degenerated acini cells and islet of Langerhans (\*\*\*) and presented different alterations of rat's pancreas and many histological changes were detected in pancreas section of (G2) that administrated by dexamethasone, such as necrosis and damage of endocrine cells of islet Langerhans with shrinkage of islets, Dexamethasone induced necrosis is mediated by reactive oxygen species mediated lipid peroxidation which causes bursting of plasma membrane of the cell and disturbance of osmotic balance this osmotic alteration ultimately leads the cell towards necrosis.

Also the histological section show different change in pancreas of rats that administrated with dexamethasone

and CeO<sub>2</sub> Nanoparticles (G3 and G4) these change increased by decreasing the dose of Nanoparticles in which cells look like normal histological structure of pancreas with dispersed necrosis cells, the healing effect of Nanoparticles from Fig. (4 a and b) photomicrograph it is observed that the empty spaces in islets created by dexamethasone induced necrosis is significantly decreased and the section showed dispersed necrosis of endocrine cells of inside the islet of Langerhans with certain reduction the contour of islets and ballooning degenerate of cytoplasm of cells; this indicates that Nanoparticles stimulates the regeneration of the damaged islets, from Fig. (4c and d) can see that Nanoparticles kept normal shape of pancreatic cells and they look like normal.

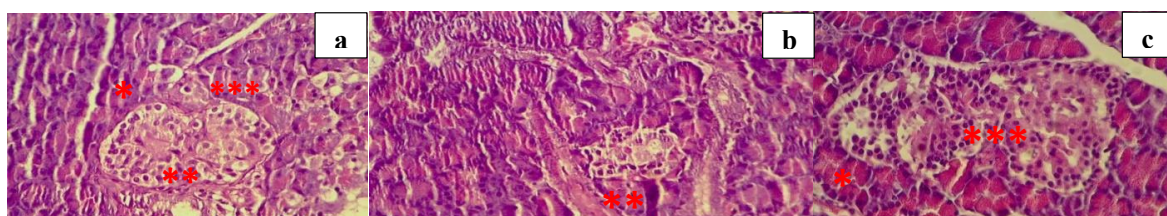


**Figure (3):** Cross section of pancreas (a) Control group, (b and c) Group 2 X400 (H&E),

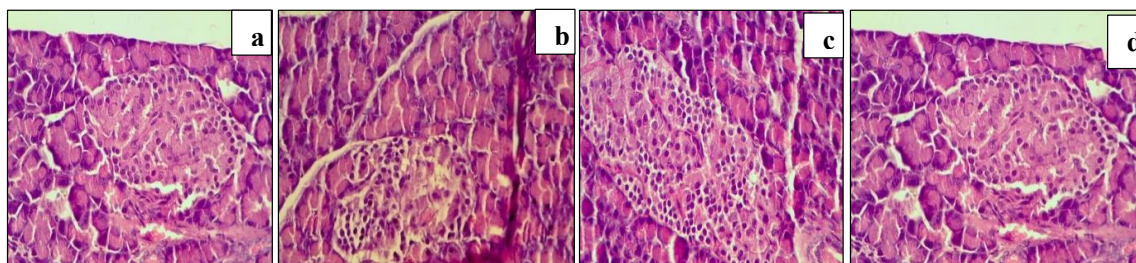


**Figure (4):** Cross section of pancreas (a) G3 (b) G4 (c) G5 (d) G6 X400 (H&E).

## Conclusions

Synthesis of biocompatible Nanoparticles was obtained by applying a novel and simple green technique using new extract of green tea (*Camellia Sinensis*) to prepare Cerium Oxide nanoparticles. It had investigated successful formation of nanoparticles by examine its structural and optical properties, nanoparticles administration provided a significant reduction against BGL after dexamethasone injection, using nanoparticles reduced serum blood glucose levels, improved Liver enzymes and Bilirubin to confirm this results the histological staining of pancreatic section have performed.

## References

1. Dijken A. V., Meulenkamp E. A., Vanmaekelbergh D., Meijerink A. Identification of the transition responsible for the visible emission in ZnO using quantum size effects. *Journal of Luminescence* 2000;90:123-128.
2. Gunalan S., Sivaraj R., Rajendran V. Green synthesized ZnO nanoparticles against bacterial and fungal pathogens *Progress in Natural Science. Materials International J.* 2013;10:1002-1016 67.
3. Etheridge M., Campbell S., Erdman A., Haynes C., Wolf S., McCullough J. The big picture on nanomedicine: the state of investigational and

- approved nanomedicine products. *Nanomedicine: Nanotechnology, Biology, and Medicine*. 2013;9:1–14.
4. Nada K. A., Anwar A. B., Nadia J. G. The effect of annealing temperature on the optical properties of (Cu<sub>2</sub>S)<sub>100</sub>-X (SnS<sub>2</sub>)<sub>X</sub> thin films. *Baghdad Science Journal*. 2014; 11(2).
  5. Harrison D., Griendling K. K., Landmesser U., Hornig B., and Drexler H. Role of oxidative stress in atherosclerosis. *American Journal of Cardiology*, 2003;91,3,7–11.
  6. Stephens J.W., Khanolkar M. P., and Bain S. C. The biological relevance and measurement of plasma markers of oxidative stress in diabetes and cardiovascular disease. *Atherosclerosis J*, 2009;202(2),321–329.
  7. Pillarisetti S., Saxena U. Role of oxidative stress and inflammation in the origin of Type 2 diabetes a paradigm shift *Expert Opinther Targets*. 2004;8:8–401.
  8. Xiangqian L., Huizhong X., Zhe-Sheng C., and Guofang C. Biosynthesis of nanoparticles by microorganisms and their applications. *Journal of Nanomaterials*, 2011;Article 270974, p16.
  9. Ahmed S., Ahmad M., Swami B. L., and Ikram S. A review on plants extract mediated synthesis of silver nanoparticles for antimicrobial applications: a green expertise. *Journal of Advance Research*. 2016;7,17-28.
  10. Karakoti A., Singh S., Dowding J.M., Seal S., Self W.T. Redox-active radical scavenging nanomaterials. *Chem. Soc. Rev*. 2010;39:4422–4432.
  11. Ogawa A., Johnson J.H., Ohneda M., McAllister C.T., Inman L., Alam T., and Unger R.H. Roles of Insulin Resistance and  $\beta$ -Cell Dysfunction in Dexamethasone-induced Diabetes. *the journal of clinical investigation*, 1992; 90(2):497–504.
  12. Ohneda M., Inman L. R., and Unger R. H. GLUT-2 function in glucose-unresponsive beta cells of dexamethasone-induced diabetes in rats. *the journal of clinical investigation*, 1993;92(4):1950–1956.
  13. K. T., Koo K. H., and Park J. S. Toxicological Evaluations of Rare Earths and Their Health Impacts to Workers : A Literature Review. 2013;12–26.
  14. Bancroft JD, Gamble M. *Theory and Practice of Histological Technique*. 4th Ed.; Churchill: Livingston, NY, USA, 2008.
  15. Munusamy S., Bhakayaraj K., Vijayalakshmi L., Stephen A., and Narayanan V. Synthesis and characterization of cerium oxide nanoparticles using *Curvularia lunata* and their antibacterial properties. *Int J Innov. Res Sci Eng*, 2014; 2(1):318–323.
  16. Priya G. S., Kanneganti A., Kumar K. A., Rao K. V., and Bykkam S. Bio Synthesis of Cerium Oxide Nanoparticles using *Aloe Barbadosis* Miller Gel. *Int. J. Sci. Res. Publ*. 2014; 4(1):2250–3153.
  17. Alkauskas A., Pasquarello A. Band-edge problem in the theoretical determination of defect energy levels: The O vacancy in ZnO as a benchmark case. *J. Phys. Rev. B*. 2011;84-125206.
  18. Maqbool Q., Nazar M., Naz S., Hussain T., Jabeen N., Kausar R., Anwaar S., Abbas F. and Jan T. Antimicrobial potential of green synthesized CeO<sub>2</sub> nanoparticles from *Olea europaea* leaf extract. *Int. J. Nanomed.*, 2016;5015–5025.
  19. Karmakar R., Chatak S., Haidar A., Bhattacharya S. Prednisolone-induced alteration in hepatic and muscular protein and glycogen level. Its correlation with blood glucose level in mice. *Folia Biol. Prague*. 1998;44(6):217-225.
  20. Robert E., Post M.D., Arch M.S., Mainous G., Dana King E., and Simpson K. N. Dietary Fiber for the Treatment of Type 2 Diabetes Mellitus: A Meta-Analysis. 1991;25(1), 14 :1126-1131.
  21. Noor H., Hammands P., Sutton R. and Ashcroft S. The hypoglycaemic and insulinotropic activity of *Tinospora crispa* : studies with human and rat islets and HIT-T15 B cells. *Diabetolo*. 1989;32:354-359.
  22. Kaka M., Miura T., Vsami M., Kato A. and Kadowaki. S. Hypoglycemic effect of the rhizomes of *ophiogonis tuber* in normal and diabetic mice. *Biol. Pharm. Bull*. 1995;18, 875-887.
  23. Tapa B. R., Wilia A. Liver function tests and their interpretation”, *Ind. J. Pediatr*. 2007;74(7):66-671.
  24. Hadi N. R., Al-Amran F.G., Swadi A. Metformin ameliorates methotrexate- induced hepatotoxicity. *J.Pharmacol Exp. Ther*. 2012;3(3):248-253.
  25. Hirst S.M., Karakoti A.S., Tyler R.D., Sriranganathan N., Seal S., Reilly C.M. Antiinflammatory properties of cerium oxide nanoparticles. *Small* 5, 2009; 2848–2856. doi:10.1002/sml.200901048.
  26. Cassim L. melatonin and anticancer therapy: interaction with 5-fluorouracil. PhD thesis, Rhodes university, pp.225, 2007.